

## A-1.1 Behaviors of Polar Vortices and Their Effects on Ozone Depletion

**Contact person** Hiroshi KANZAWA  
Head, Atmospheric Physics Section  
Atmospheric Environment Division  
National Institute for Environmental Studies  
Environment Agency of Japan  
16-2, Onogawa, Tsukuba, Ibaraki 305-0053, Japan  
Tel: +81-298-50-2431 Fax: +81-298-51-4732  
E-Mail: kanzawa@nies.go.jp

**Total Budget for FY1996-FY1998** 127,044,000 Yen (FY1998; 40,166,000 Yen)

**Abstract** The 1996/97 Arctic vortex was unusual in that it formed late and remained late in spring, and in that it brought record low column ozone in spring. Chemical ozone loss in the Arctic stratospheric vortex in February and March 1997 is estimated using ozone data of ILAS and ozonesonde. Both analyses show that the integrated ozone loss showed its maximum in the lower stratosphere with about 50 % loss during the two months from February to March 1997. The analyses of total reactive nitrogen ( $\text{NO}_y$ ) and nitrous oxide ( $\text{N}_2\text{O}$ ) data obtained by balloon experiments in the Arctic in February 1997 show that the effect of dynamical processes must be taken into account in quantitatively assessing the degree of denitrification and ozone loss, especially at high altitudes with  $\text{N}_2\text{O}$  values lower than 120 ppbv. A vertical sandwich structure of Type I PSCs, in which layers of relative depolarization are above and below a scattering layer, has frequently been observed in the Arctic by lidar when the stratospheric temperature decreases to near the frost point of ice, and the mechanism of its formation is discussed. A high-sensitive *in situ* ClO measurement system for balloons and aircraft was developed using the principle based on chemical reactions and a resonance fluorescence technique, and a prototype model made was sufficient for the detection of stratospheric ClO radicals. Other various observational studies were made.

**Key Words** Polar vortex, Stratosphere, Ozone decrease, Denitrification, Dynamical mixing, PSC, Balloon observation, Satellite observation

### 1. Introduction

It was reported in 1980's that ozone depletion of large scale known as the "Ozone Hole" occur in the Antarctic stratospheric polar vortex in austral winter and spring. The ozone destruction is considered to occur as results of chemical reactions involving chlorine and bromine that originate in anthropogenic compounds such as chlorofluorocarbons under the special meteorological conditions of the polar vortex. In recent years, a considerable ozone depletion has also been observed inside the Arctic polar vortex in winter and spring.

The ozone decrease in the polar stratospheric winter and spring has close relationship with the polar vortex in the same season. Because the strength, spatial scale, and position of the polar vortex have day-to-day and interannual variations, the variations affect the strength, area, and position of the ozone depletion through degrees of coldness of temperature, area of the cold temperatures, etc., inside of the polar vortex. In fact, in recent several years, large amount of ozone decrease is observed due to strong and persistent polar vortices. It is urgent to clarify the role in ozone depletion of the polar vortex which has 3-dimensional structures and which is thus not expressed by the 2-dimensional models conventionally used for projecting behavior of the ozone layer in future on the order of several ten years.

## 2. Research Objective

The final goal of the research project is to understand quantitatively the role of polar vortices in ozone chemical depletion processes.

## 3. Research Method

Various measurements of the ozone layer were made in the Arctic and Antarctic areas in coordination with observations by a satellite-borne sensor, ILAS (Improved Limb Atmospheric Spectrometer). Obtained data were analyzed for the purpose. An instrument to measure ClO was also developed. Details of the methods are shown in subsections of Section 4.

## 4. Results and Discussion

### 4.1 Chemical ozone loss in the Arctic stratospheric polar vortex using ILAS and ozonesonde data

**Summary:** The 1996/97 Arctic vortex was unusual in that it formed late, remained well defined until late in April, and was more zonally symmetric than in previous years. It was also characterized by record low temperatures and a large region of record low column ozone centered around the north pole. Chemical ozone loss in the Arctic stratospheric vortex in February and March 1997 is estimated using Version 3.10 data of ILAS (Improved Limb Atmospheric Spectrometer) (Sasano et al., 1999c) and ozonesonde data (Kreher et al., 1999). The integrated ozone loss from ILAS data showed its maximum of  $1.5 \pm 0.2$  ppmv at the surface that followed the diabatic descent of the air parcels and reached the potential temperature surface of 425 K (~17 km in altitude) level on 31 March 1997: The rate of loss is about 0.75 ppmv/month. On the other hand, from ozonesonde data over Kiruna, Sweden, the ozone loss rates of up to 0.63 ppmv/month were found inside the Arctic vortex at surfaces descending from approximately 475 K (~19 km) on 1 February to 460 K (~18.4 km) on 25 March. Both analyses show that the integrated ozone loss showed its maximum in the lower stratosphere with about 50 % loss during the two months from February to March 1997. The cause of the small difference between the two estimates is not well known. The possible causes might be as follows: (i) The ozonesonde analysis used long-term observation data made at a particular single location, thus likely reflecting the combined effects of transport and chemistry on the derived ozone loss amounts; (ii) The altitude registration problem in the ILAS data processing algorithm Version 3.10 might be also one of the causes; (iii) The treatment of incorporating the effect of diabatic descent might be an error source of the estimates.

#### (1) ILAS observations of chemical ozone loss in the Arctic stratospheric vortex in February and March 1997

**Summary:** Chemical ozone loss rates were estimated for the Arctic stratospheric vortex by using ozone profile data (Version 3.10) obtained ILAS for the spring of 1997. The analysis method is similar to the Match technique, in which an air parcel that the ILAS sounded twice at different locations and at different times was searched from the ILAS data set, and an ozone change rate was calculated from the two profiles. A statistical analysis indicates that the maximum ozone loss rate was found on 450 K (~18 km) in February, amounting to 85 ppbv/day. The integrated ozone loss for two months from February to March 1997 showed its maximum of  $1.5 \pm 0.2$  ppmv at the surface that followed the diabatic descent of the air parcels and reached the 425 K (~17 km) level on 31 March. This is about 50 % of the initial (1 February) ozone concentration.

#### (i) Background

To clearly discriminate chemical ozone destruction due to reactions involving chlorine and bromine that originate in anthropogenic compounds such as chlorofluorocarbons from

dynamical ozone changes caused by advection and mixing through the vortex boundary, the group of von der Gathen applied a new technique called "Match" to a data set of ozone sonde measurements, i.e., calculated the amount of ozone change in an air parcel that has passed two separate locations inside the polar vortex so that dynamic effects can be neglected and only chemical changes remain. It is quite natural to apply the similar technique to ozone profile data obtained with satellite-borne sensors. The Improved Limb Atmospheric Spectrometer (ILAS) developed by the Environment Agency of Japan (EA), and on board the Advanced Earth Observing Satellite (ADEOS) which was launched by the National Space Development Agency of Japan (NASDA) is described in Sasano et al. (1999b) and in the ILAS home page (<http://www-ilas.nies.go.jp/>). It made intensive measurements over high-latitude stratospheres, totaling 731 sunrise events over a relatively narrow latitude range of 67 to 70 degrees N during the period from February to March in the Arctic Spring of 1997, when a relatively distinct polar vortex was persisting. Therefore, a number of air parcels are likely to have been unintentionally sounded at different ILAS measurement locations, and consequently there is a sufficient number of coincidences to apply the Match analysis.

## (ii) Results and discussion

Ozone change rates per day for sunlit time as a function of potential temperature and date in the polar vortex were estimated. The polar vortex was defined using UKMO Ertel's potential vorticity (EPV) and wind fields as shown below in Section 4.1(2). The local maximum ozone loss rate is found on the 450 K surface (~18 km) in the latter half of February, amounting to about 85 ppbv/day. Significant negative regions correspond well to those for PSCs appearance as well as for very low temperature. This strongly suggests that a well-recognized ozone destruction mechanism acted on the air parcels, in which generation of PSCs, activation of chlorine species due to heterogeneous reactions on PSC surfaces, and chain reaction that destroyed ozone under a sunlit condition occurred in sequence. The integrated ozone loss from day 29 (1 February) to day 90 (31 March) showed its maximum of 1.5 +/- 0.2 ppmv on the surface that reached the 425 K (~17 km) level on 31 March from the 457 K (~18.3 km) level on 1 February due to the diabatic descent of the air parcels. This is about 50 % of the initial (1 February) ozone concentration.

An analysis was made by Knudsen et al. (1998) using ozone sonde data obtained at many locations and accounting for horizontal transport by assessing the exchange of air parcels across the vortex edge with domain filling trajectory calculations. They reported ozone decreases of 1.45 ppmv, 1.59 ppmv, 1.24 ppmv, and 1.20 ppmv for the period from 6 January to 6 April for the air masses on 425 K, 450 K, 475 K, and 500 K potential temperature surfaces at the end of the period, respectively. The chemical ozone loss at the 425 K surface estimated as 1.5 ppmv in our case agrees well with the results by Knudsen et al. (1998).

The present study has derived quantitatively the chemical ozone loss rates as a function of altitude (potential temperature) and date from the analysis of ozone changes in the same air parcels observed by a satellite-borne solar occultation sensor. It was demonstrated that satellite sensor data that, in general, has a vertical resolution of 1 - 2 km could be applied to such an analysis. Since a polar orbital solar occultation sensor such as ILAS can intensively measure high-latitude regions, it can provide a very useful data set for an analysis such as presented in this paper. In addition, ILAS provides data on not only ozone but also other chemical species such as nitric acid, nitrous oxide, methane, water vapor, and aerosol extinction coefficients obtained at the same time and at the same location. This means further comprehensive analysis is possible especially on ozone depletion mechanisms involving heterogeneous reactions on the surfaces of polar stratospheric clouds. For example, N<sub>2</sub>O and HNO<sub>3</sub> correlation plots from ILAS data indicated that denitrification processes played an important role in the ozone decrease.

## (2) Ozone sonde observations of chemical ozone loss in the Arctic stratospheric vortex in February and March 1997

Summary: Ozone depletion above Kiruna (67.9 N, 21.1 E), Sweden, was investigated using daily ozone and temperature measurements by ozonesondes between 1 February and 25 March 1997. Using UKMO Ertel's potential vorticity (EPV) and wind fields, three dynamically

distinct regions were defined on a grid of isentropic surfaces viz.: the polar vortex boundary region characterized by steep EPV gradients, the area poleward of the boundary region (inside the polar vortex), and the area equatorward of the boundary region (outside the polar vortex). Due to dynamically induced displacements of the vortex, measurements were made in all three regions. By calculating the isentropic EPV at each measurement point and comparing it with the values defining the equatorward and poleward edges of the vortex boundary region, all ozone and temperature measurements could be binned according to their position relative to the vortex edge. Since the data outside the polar vortex were highly variable, mean ozone profiles and their standard deviations were calculated and compared only for the two other regions. To investigate whether differences between these mean profiles were indicative of ozone loss, the temporal evolution of ozone mixing ratios measured along several isentropic surfaces was examined, taking into account the diabatic descent of airmasses. Finally, ozone loss rates were calculated for six potential temperature surfaces and loss rates of up to 0.63 ppmv/month were found inside the Arctic vortex at surfaces descending from approximately 475 K (~19 km) on 1 February to 460 K (~18.4 km) on 25 March.

#### (i) Background

During the unusual Arctic winter, 55 ozonesonde flights were made from ESRANGE, Kiruna, during February and March 1997 as part of the ILAS validation balloon campaign (Kanzawa et al., 1997). The ozone and temperature profiles measured during these flights were used to investigate the altitude range above Kiruna where ozone depletion may have occurred. To this end, each ozone and temperature value measured along the ozonesonde flight path was binned according to its position relative to the polar vortex, i.e., if it was measured inside the vortex, in the vortex boundary region, or outside the vortex. The differences between the mean profiles calculated for ozone values inside the polar vortex and in the vortex boundary region and their temporal evolution for airmasses including diabatic descent are discussed. The observed ozone mixing ratio trends are then used to infer ozone depletion rates above Kiruna.

#### (ii) Results and Discussion

Stratospheric temperatures above Kiruna were predominantly controlled by the position of the polar vortex in such a way that cold temperatures were located inside the polar vortex. During three periods, day 40 to 42, day 51 to 57, and day 66 to 67, temperatures fell below 195 K, taken as the condensation threshold for Type I ( $\text{HNO}_3$  and  $\text{H}_2\text{O}$ ) PSCs.

The vortex boundary region acts as a barrier to horizontal transport, isolating the interior of the vortex from midlatitude airmasses. Furthermore, as a result of the steep EPV gradients in the vortex boundary region, which restrict transport, there is also only little intrusion of midlatitude air into the vortex boundary region. Therefore, it is safe to assume that both the vortex interior and vortex boundary region are isolated from lower latitude air intrusion. This assumption is valid for the Antarctic vortex and since the 1996/97 Arctic vortex was in some respect dynamically similar to an Antarctic vortex, it is probably also true for the Arctic vortex.

To investigate whether differences between the mean profiles were indicative of ozone loss and to determine the ozone loss rate inside the polar vortex, the temporal evolution of ozone inside the vortex and in the vortex boundary region was examined. The measured ozone mixing ratios were interpolated onto selected isentropic surfaces following the diabatic descent of the airmasses inside the vortex. The diabatic descent rates during February and March 1997 were calculated from modelled cooling/heating rates and then integrated over the area of the vortex interior to obtain the mean descending motion [private communication, M. Rex and M. Chipperfield]. The decrease in ozone observed on the potential temperature was between 0.2 - 0.6 ppmv/month inside the Arctic vortex and 0.4 - 0.6 ppmv/month in the boundary region. The most pronounced ozone loss above Kiruna is observed inside the vortex on surfaces descending from 475 +/- 10 K (~19 km) on 1 February to 460 +/- 10 K (~18.4 km) on 25 March, amounting to 18 - 21 ppbv per day or 0.54 - 0.63 ppmv per month. These results are in good agreement with the chemical ozone depletion found by Knudsen et al. (1998).

## 4.2 Dynamical mixing and denitrification in the Arctic stratospheric polar vortex observed by balloon experiments

Summary: Denitrification can delay the deactivation of chlorine, leading to extended ozone depletion throughout the winter and early spring. Denitrification was observed inside the Arctic vortex in mid-February 1995. The balloon data in February 1997 showed that between 500 K (~20 km) and 600 K (~24 km), the  $N_2O$  values were lower than 120 ppbv and the observed  $NO_y$  values were some 4-6 ppbv lower than those calculated using the midlatitude  $NO_y$ - $N_2O$  correlation which includes the  $NO_y$  reduction due to the  $N + NO$  reaction. The temperatures in the Arctic winter above the 550 K level were too high to cause extensive denitrification. The combined processes of diabatic descent and quasi-horizontal mixing of vortex air are likely causes of the anomalous  $NO_y$ - $N_2O$  correlation. The effect of dynamical processes must be taken into account in quantitatively assessing the degree of denitrification and ozone loss, especially at high altitudes with  $N_2O$  values lower than 120 ppbv.

### (i) Background

The correlation between  $NO_y$  ( $NO_y = NO + NO_2 + HNO_3 + 2(N_2O_5) + HO_2NO_2 + ClONO_2 + BrONO_2 + \text{aerosol nitrate}$ ) and  $N_2O$  is a suitable tool to investigate the chemical and dynamical processes that affect stratospheric  $NO_y$ . In particular, irreversible loss of  $NO_y$  due to sedimentation of  $HNO_3$ -containing particles inside the winter polar vortices (denitrification) has been quantitatively estimated using  $NO_y$ - $N_2O$  correlations unperturbed by denitrification (Sugita et al., 1998). Denitrification can delay the deactivation of chlorine, leading to extended ozone depletion throughout the winter and early spring.

Previous observations of  $NO_y$  and  $N_2O$  mixing ratios at midlatitudes have shown very tight linear correlations up to 30 km where their chemical lifetimes are much longer than their transport times. At midlatitudes above 33 km, where  $N_2O$  mixing ratios are lower than 50 ppbv, the  $NO_y$  values have been observed to be significantly lower than those predicted from a linear extrapolation of the observed correlations due to the net loss of  $NO_y$  in the upper stratosphere (Sugita et al., 1998) due to the following reactions:



Whether the  $NO_y$ - $N_2O$  relationship obtained at midlatitudes holds inside the polar vortex in the absence of denitrification is not yet clear due to the insufficient simultaneous measurements of  $NO_y$  and  $N_2O$ . In particular, observations of  $NO_y$ - $N_2O$  correlations at  $N_2O$  mixing ratios lower than 50 ppbv are very scarce inside the Arctic and Antarctic vortices, since  $N_2O$  levels are rarely significantly lower than 50 ppbv below 20 km, which is the maximum altitude of the ER-2 aircraft measurements. Simultaneous observations of  $NO_y$  and  $N_2O$  were made by Atmospheric Trace MOlecule Spectroscopy (ATMOS) on board the space shuttle during the Atmospheric Laboratory for Applications and Science (ATLAS) 2 mission inside the Arctic vortex in April 1993, when the vortex was defined below the potential temperature of 800 K. Balloon-borne measurements of  $NO_y$  and  $N_2O$  were made in the Arctic stratosphere in February 1997 to elucidate  $NO_y$ - $N_2O$  correlations inside the stable vortex in mid-winter. The observed  $NO_y$ - $N_2O$  correlations are interpreted in terms of transport and chemical processes as described in Kondo et al. (1999).

### (ii) Results and Discussion

Balloon-borne *in situ* measurements of the concentrations of  $NO_y$ ,  $N_2O$ , and aerosol were made from Kiruna, Sweden (68 N, 21 E) on 970210 (10 February 1997) and 970225 (25 February 1997) as part of the ILAS validation balloon campaign (Kanzawa et al., 1997). On 970210, Kiruna was located at the edge of the vortex at 475 and 550 K and inside the vortex at 675 K. Kiruna was inside the vortex between 475 K and 675 K on 970225.

Below 500 K (~20 km), the  $N_2O$  levels were higher than 120 ppbv on both days. The  $NO_y^*$  values calculated from the observed  $N_2O$  mixing ratios using the northern midlatitude  $NO_y$ - $N_2O$  correlation agreed well with the observed  $NO_y$  values, except at 435-455 K (18.4±0.5 km) on 970225. Back trajectory calculations show that the air masses in a narrow altitude region of 435-460 K experienced temperatures closest to  $T_{ICB}$ , suggesting that the low

NO<sub>y</sub> values observed between 435 K and 455 K were caused by denitrification.

At higher altitudes between 500 K (~20 km) and 600 K (~24 km), the observed NO<sub>y</sub> values were 4-6 ppbv lower than the NO<sub>y</sub>\* values on both days. It is unlikely that these lower NO<sub>y</sub> values were also caused by denitrification given that the minimum temperatures in the Arctic at these altitudes did not reach T<sub>ICE</sub> during the winter. Above 33 km at midlatitudes, N<sub>2</sub>O values are typically lower than 50 ppbv and the NO<sub>y</sub>-N<sub>2</sub>O correlation becomes non-linear at these altitudes. The NO<sub>y</sub> mixing ratios are much lower than those expected from the linear extrapolation of the NO<sub>y</sub>-N<sub>2</sub>O correlation obtained at N<sub>2</sub>O values higher than 120 ppbv. Diabatic descent of air masses low in N<sub>2</sub>O deep inside the vortex, followed by mixing with air with higher N<sub>2</sub>O values from the vortex edge should result in an NO<sub>y</sub>-N<sub>2</sub>O correlation different from that prevailing prior to the mixing. In support of this hypothesis, air masses with N<sub>2</sub>O mixing ratios of 4-17 ppbv and NO<sub>y</sub> mixing ratios lower than 13 ppbv were sampled during the balloon observations deep inside the Arctic vortex at potential temperatures between 600 K and 780 K in the winters of 1994-1995 and 1996-1997. These air masses were transported from the upper stratosphere retaining the midlatitude NO<sub>y</sub>-N<sub>2</sub>O correlation. The low N<sub>2</sub>O values indicate that descended air masses were mixed quasi-horizontally only with air masses with comparably low N<sub>2</sub>O values deep inside the vortex, where the N<sub>2</sub>O gradient was weak. This mixing will not significantly alter the NO<sub>y</sub>-N<sub>2</sub>O correlation, since the correlation at midlatitudes is almost linear for these low N<sub>2</sub>O values.

At lower altitudes between 500 K and 600 K, the NO<sub>y</sub>-N<sub>2</sub>O correlation of the descended air masses was significantly influenced by quasi-horizontal mixing within the vortex, leading to the apparent deficit in NO<sub>y</sub> for N<sub>2</sub>O values lower than 120 ppbv. Since the NO<sub>y</sub>-N<sub>2</sub>O correlation in the N<sub>2</sub>O region between 4 and 50 ppbv is highly non-linear, mixing of upper stratospheric air with lower stratospheric air with much higher N<sub>2</sub>O values alters NO<sub>y</sub>-N<sub>2</sub>O correlation. In addition, the CH<sub>4</sub>-N<sub>2</sub>O correlation observed inside the Arctic vortex on 970211 and 970222 also deviated from that observed at midlatitudes by ATMOS-ATLAS 3, indicating that air masses with N<sub>2</sub>O values as low as 5-10 ppbv descended and mixed with lower stratospheric air in which the midlatitude CH<sub>4</sub>-N<sub>2</sub>O correlation had prevailed prior to the mixing.

Given that the NO<sub>y</sub> values were lower than those expected from the midlatitude NO<sub>y</sub>-N<sub>2</sub>O correlation at N<sub>2</sub>O values of 20-120 ppbv in the Arctic winters of 1991-1992, 1992-1993, and 1996-1997, dynamical processes likely altered the NO<sub>y</sub>-N<sub>2</sub>O correlation inside the vortex for each winter. The effect of dynamical processes must be taken into account in quantitatively assessing the degree of denitrification, especially at N<sub>2</sub>O values lower than 120 ppbv.

#### 4.3 PSCs (Polar Stratospheric Clouds) observations by lidar

Summary: A vertical sandwich structure of Type I PSCs, in which layers of relative depolarization are above and below a scattering layer, has frequently been observed by lidar at Ny-Ålesund, Svalbard (79 N, 12 E) when the stratospheric temperature decreases to near the frost point of ice. The main difference between the temperature history of PSCs in the scattering layer and those in the depolarization layer was the temperature at which the structure is observed. The small increase in the scattering ratio over time at the altitude of the depolarization maximum implies a slow nucleation of solid particles, and suggests that the sandwich structure arises from the external mixing of two different types of particles. A large fraction of liquid particles, grown at low temperature, constitutes the scattering layer, while at higher temperatures, a very small fraction of solid particles is responsible for the depolarization layer.

##### (i) Background

Type I PSCs are assumed to form via the absorption of nitric acid molecules from the atmosphere. However, since *in situ* measurements of the composition and phase of these particles are still very difficult to perform, their microphysical properties are not well known despite the many efforts involving field observations and laboratory experiments. Although PSC particles in the solid phase have been observed via lidar in early studies on PSCs, the conditions required for the phase transition from liquid to solid particles (or from sulfuric-acid background aerosols to solid PSCs), are still not clear. Lidar can accurately determine the

vertical distribution of PSCs. Spherical and aspherical particles can be detected and distinguished by lidar via depolarization measurements. These spherical particles are interpreted to be liquid particles. With these capabilities, lidar is a powerful tool for studying the microphysical properties of PSC particles. Shibata et al. (1997) reported the results of lidar observations in the winter of 1994/1995 in Svalbard, and found a vertical “*sandwich structure*” in which a liquid PSC layer was situated between solid PSC layers when the lowest temperature had been near  $T_{ice}$  during January 1995. *Sandwich structures* were often seen when the temperature decreased to near  $T_{ice}$  during subsequent winters.

This research reviews typical cases of PSC events with sandwich structures, and it obtains characteristic temperature histories of these PSC particles by back trajectory analysis utilizing Global Objective Analyses Data of the Japan Meteorological Agency. The mechanism responsible for the formation of a *sandwich structure* and the mixing state of PSC particles is proposed.

#### (ii) Research Method

Three parameters of lidar observed PSC particles are used to examine the sandwich structure: (1) The scattering ratio  $R = (\beta_M + \beta_A) / \beta_M$ , where  $\beta_M$  is the backscattering coefficient of atmospheric molecules, and  $\beta_A$  is the backscattering coefficient of aerosols. (2) The depolarization ratio  $\delta = \beta_s / (\beta_p + \beta_s)$  where  $\beta_p$  and  $\beta_s$  are the parallel and perpendicular components of the signal, respectively. (3) The Angstrom exponent  $\alpha$  is calculated using two harmonically related wavelengths of 532 nm and 1064 nm of the lidar with the assumption that  $\beta_A \propto \lambda^{-\alpha}$ . The temperature histories are calculated from Global Objective Analyses Data of the Japan Meteorological Agency.

#### (iii) Results and Discussion

Typical sandwich structures were observed on 10 January 1995, 6 January 1996, and 20 February 1997. The characteristics of the temperature history of PSC particles can be summarized as follows: (i) When the sandwich structure is observed, the temperatures relative to  $T_{ice}$  at the  $R$ -layer, defined as a layer with large  $R$ , are 1-3 K lower than the temperatures at the  $\delta$ -layers, defined as a layer with large  $\delta$ ; (ii) The averages and deviations of the temperature histories as well as the cooling rate histories of PSCs in the  $R$ - and  $\delta$ -layers are similar; (iii) Only a few out of PSC layers experienced a temperature lower than  $T_{ice}$  before the PSC particles arrived over Ny-Ålesund.

At the 532-nm wavelength, the scattering ratio  $R$  in the presence of PSCs has been found to increase up to a value of about 2 as  $\delta$  increases. As the value of  $R$  increases above 2,  $\delta$  decreases and approaches 0. This inverse correlation between  $\delta$  and  $R$  is characteristic of type Ia and type Ib PSCs. There is a drastic increase in the saturation ratio of these PSC particles when the phase of the particles changes from liquid sulfuric acid or ternary solution to solid nitric-acid hydrates like NAT. If most of the background sulfate aerosols change from the liquid to the solid phase, since the saturation ratio of the particles also increases, all the solid particles would grow rapidly until the partial pressure of source gases balances the saturation vapor pressure of the solid particles. Under these conditions, the majority of  $HNO_3$  molecules would rapidly be absorbed by the solid particles, and the ratio  $R$  at 532 nm can become much larger than 2.

The exponent  $\alpha$  would now be smaller than that of the background aerosols where  $\delta$  is large because of the introduction of larger-grown particles relative to the background ones (Shibata et al., 1997). However, since a rapid increase in  $R$  does not accompany the increase in  $\delta$ , the number concentration of solid PSC particles appears to be much smaller than that of the liquid background particles. In other words, if the nucleation rate of solid particles from the liquid is sufficiently small, then most of the background aerosol would still be in the liquid phase when the solid PSCs are detected with lidar. This interpretation is consistent with observations in laboratory experiments in which background liquid aerosols do not readily freeze in polar stratospheric conditions.

When the ambient temperature drops near  $T_{ice}$ , the  $R$ -increase with accompanying  $\delta$ -diminution of the sandwich structure is observed. Consider the conditions described above (a small number of solid hydrates of nitric acid particles externally mixed with a large number of liquid particles). The mechanism whereby  $\delta$  first increases without a concomitant increase in  $R$  during cooling, followed by an increase in  $R$  with decreasing  $\delta$  at the lower temperature, can be understood. If a small number of particles are solid at a temperature lower than the condensation point temperature of the solid composite, they will rapidly grow to a large size. These nucleating solid particles increase the depolarization while only minimally increasing  $R$ . When the temperature drops further with a small number of frozen particles, the liquid particles grow by absorbing nitric acid and water molecules to form a ternary solution. Since most of the particles are liquid, they effectively increase backscattering of the mixture and thus decrease  $\delta$ . Near the altitude of lowest relative temperature ( $T - T_{ice}$ ), the increased backscattering by the liquid particles will begin reducing  $\delta$  whose increase had been dominated by the solid particle number. On either side of this lowest-temperature altitude region, there are temperature regions where the growth of liquid particles is not sufficient to increase  $R$  and decrease  $\delta$ . The sandwich structure is observed under these conditions.

#### 4.4 Measurements of $O_3$ and $N_2O$ with a TDLHS (tunable diode laser heterodyne spectrometer)

Summary: A trial to estimate the chemical ozone depletion over Alaska during the spring season of 1997 is made from the profiles of  $O_3$  and  $N_2O$  observed with TDLHS.

##### (i) Background

The correlation analysis between chemically active species (e.g.,  $O_3$  or HCl) and quasi-inert trace species (e.g.,  $N_2O$ ,  $CH_4$ , or HF) is useful to separate chemical changes from variations due to dynamical processes. We try to examine the chemical ozone depletion over Alaska during the spring season of 1997 from the profiles of  $O_3$  and  $N_2O$  observed with TDLHS (Murata et al., 1999).

The TDLHS was developed at Tohoku University. This spectrometer can measure individual atmospheric absorption spectra with a spectral resolution of  $0.0013 \text{ cm}^{-1}$  and a signal-to-noise ratio of 500 for a single 10-minute scan. The observations were carried out at Poker Flat Research Range, Geophysical Institute, University of Alaska Fairbanks (65 N, 147 W), from 17 February to 10 March and from 1 April to 8 May 1997. Data were taken on 32 clear days. The vertical profiles of  $O_3$  and  $N_2O$  volume mixing ratios were derived with an inversion method.  $O_3$  was retrieved for an altitude range of 7 to 25 km and  $N_2O$  for 9 to 25 km. The altitude resolution is about 5 km. Poker Flat was usually located outside the polar vortex during the observational period from early to late spring, but sometimes located inside the vortex as in the cases of 10 March and 17 April 1997.

##### (ii) Results and discussion

The  $O_3$  volume mixing ratio is larger at altitudes above 11 km on 10 March than that on 4 March. The  $N_2O$  volume mixing ratio observed on the same days is smaller between 11 and 21 km on 10 March than that on 4 March. According to the potential vorticity maps, the airmass over Poker Flat was located outside the polar vortex in all altitude region on 4 March. On the other hand, it was located outside the polar vortex in the altitudes higher than 475 K (about 19 km altitude) in potential temperature but located in the boundary region of the vortex in the altitudes around 435 K (about 17 km) and located inside the vortex in the altitudes between 380 K (about 14 km) and 400 K (about 15 km) on 10 March. Backward trajectories also show that the airmasses at the 380 K and 400 K levels came from higher latitudes. The observed profiles show that  $O_3$  volume mixing ratio is larger inside the vortex than outside while  $N_2O$  volume mixing ratio has an opposite tendency. This indicates that the subsidence of the airmass was occurring inside the vortex. We can not estimate the chemical ozone loss from the ozone profiles alone because of dynamical effects as above.

The correlation plots between O<sub>3</sub> and N<sub>2</sub>O are useful to eliminate the dynamical effect. If the variations of O<sub>3</sub> and N<sub>2</sub>O are only due to subsidence of the airmass, the correlation will not change between the both days in the lower stratosphere. The correlation plots show that O<sub>3</sub> volume mixing ratios on 10 March were smaller than those on 4 March between 11 and 20 km, indicating that O<sub>3</sub> inside the vortex on 10 March was chemically depleted. Actual ozone depletion might occur between 14 and 17 km.

The non-perturbed ozone amount for 10 March was calculated using the correlation plots between O<sub>3</sub> and N<sub>2</sub>O. Here "non-perturbed ozone" means the ozone amount in the case without chemical ozone loss. It was calculated using the correlation between O<sub>3</sub> and N<sub>2</sub>O on 4 March to the observed N<sub>2</sub>O volume mixing ratio on 10 March. The calculated non-perturbed ozone profile on 10 March is larger than the observed one, which means chemical ozone depletion occurred. In this case the difference in total column between the two profiles is about 120 DU. This estimation is rough because the origins of the airmasses on the two days are not the same and the mixing of the airmass is not considered. But it is suggested that large amount of chemical ozone depletion in the order of 100 DU had occurred inside the polar vortex in March 1997.

#### 4.5 Development of ClO measurement instrument for balloon and aircraft

Summary: We have developed a high-sensitive *in situ* ClO measurement system that can be carried on balloons and aircraft. The principle of ClO detection is based on chemical reactions and a resonance fluorescence technique. We have also made a prototype model of the balloon-borne ClO measurement system. The detection limit in our system is estimate to be 10<sup>6</sup> molecules/cm<sup>3</sup> in 60 seconds. This sensitivity is enough for the detection of stratospheric ClO radicals.

##### (i) Background

The concentration of ClO radicals in the stratosphere reflects the degree of the ozone destruction by CFC compounds. Therefore measurements of the global ClO distribution provide important information about the role of chlorine compounds on the O<sub>3</sub> depletion. We have developed a high-sensitive *in situ* ClO measurement system that can be carried on balloons and aircraft as briefly described in Hitsuda et al. (1999). The principle of ClO detection in our system is based on chemical reactions and a resonance fluorescence technique. The detection limit in our system is estimate to be 10<sup>6</sup> molecule/cm<sup>3</sup> in 60 seconds. The spatial resolution of our *in situ* system may be high enough to study the effects of heterogeneous reactions on such as cirrus cloud and sulfate aerosol.

Since the concentrations of stratospheric ClO radicals are in the range of 10<sup>7</sup>-10<sup>9</sup> molecules cm<sup>-3</sup> even in the perturbed polar regions, a high sensitivity is required for the detection of ClO radicals. The objectives of this research are developments of the stratospheric ClO measurement system and a prototype of the balloon-borne instrument for the ClO detection. This balloon-borne instrument can measure local concentration of ClO radicals, the results of which enable us to examine effects of inhomogeneous reactions in the ozone destruction processes.

##### (ii) Research method

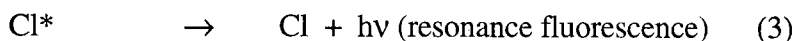
The principle of our ClO measurement system is as follows. ClO radicals in the sample air are converted to chlorine atoms by the reaction with nitric oxide (NO).



The rate of the reaction (1) is fast, that is,  $k(\text{ClO} + \text{NO}) = 1.7 \times 10^{-11} \text{ cm}^3 \text{ molecule}^{-1} \text{ s}^{-1}$ . The Cl atoms produced are excited by a chlorine lamp at 118.9 nm.



The resonance fluorescence from the excited chlorine atoms is detected.



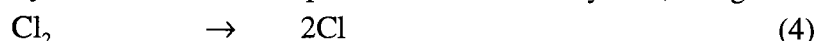
The intensity of the resonance fluorescence is proportional to the concentration of the initial ClO radicals in the sample air. The absolute concentration of ClO radicals can be derived from the

fluorescence intensity with a calibration factor of the detection system. The minimum sensitivity required for the stratospheric ClO measurements is estimated to be  $10^6$  molecules per  $\text{cm}^3$  in 60 seconds.

### (iii) Results

First, we have developed chlorine lamp at 118.9 nm which is not commercially available. The excitation source for the Cl atoms is a chlorine resonance lamp which is powered by radio-frequency discharge. The lamp is equipped with a  $\text{MgF}_2$  window and an oxygen gas filter. Although the resonance wavelength of 118.9 nm is in the vacuum UV wavelength region, it can be used in the atmospheric measurements since this wavelength corresponds to the window of oxygen absorption. The resonance fluorescence from Cl atoms excited by the lamp is monitored by a VUV photomultiplier. The calibration factor depends on the VUV emission at 118.9 nm from the chlorine lamp.

The sensitivity calibration of our system is performed using a gas flow system in the laboratory. ClO radicals were produced in the flow system, using the following reactions.



The absolute concentration of Cl atoms were obtained by absorption measurements. The signal intensities of both the resonance fluorescence and the absorption of the 118.9 nm lamp flux are simultaneously detected. The sensitivity factor  $C$  is determined from the expression,

$$C = \text{DS}_{\text{Cl}} / [\text{Cl}], \quad (6)$$

Where  $\text{DS}_{\text{Cl}}$  is the difference between the fluorescence detector count rates in the presence and absence of Cl, and  $[\text{Cl}]$  is absolute concentration of chlorine atoms. The fluorescence intensity was plotted versus chlorine atom concentration. The slope of the plots corresponds to the sensitivity factor  $C$ . The slope value of  $C = 1 \times 10^{-6} (\text{count s}^{-1}) / (\text{atom cm}^{-3})$  was obtained by the least square fitting to the plots.

### (iv) Discussion

The sensitivity factor of the developed system was  $C = 1 \times 10^{-6} (\text{count s}^{-1}) / (\text{atom cm}^{-3})$ . The background signal intensity due to wall reflection and Rayleigh scattering was about 10-100 counts / s. The detection limit of our system is estimated to be  $10^6$  molecules/ $\text{cm}^3$ , when the cycle time is about 60 s for the practical ClO measurement in the stratosphere. This sensitivity is enough to measure the stratospheric ClO radical concentrations. The dissipation of chlorine atoms in the flow tube was observed after the ClO radicals were converted to Cl atoms by addition of NO gas. This is due to the wall reaction of chlorine atoms. The mixing point of NO gas in the flow tube was optimized to get a maximum detection sensitivity.

## 4.6 Others

Ground-based measurements of ozone and ozone-related atmospheric minor constituents with FTS (Fourier Transform Infrared Spectrometer) were made at Kiruna (68 N, 21 E). Algorithm studies to derive many species from the FTS data were developed.  $\text{HNO}_3$  data turned out to be useful for validating ILAS  $\text{HNO}_3$  data. Ozonesonde data at Syowa (69 S, 40 E) gave useful data for the Antarctic ozone hole phenomena, and in addition for validating ILAS  $\text{O}_3$  data as shown in Sasano et al. (1999a). UV-visible spectrometer measurements of column amount of  $\text{O}_3$  and  $\text{NO}_2$  were continued at Kiruna (68 N, 21 E), Syowa (69 S, 40 E), and Arrival Heights (78 S, 167 E). FTS measurements were also continued at Arrival Heights (78 S, 167 E).

## References

- Hitsuda, K., N. Toriyama, Y. Matsumi, Y. Kondo (1999): Development of a balloon-borne in-situ ClO measurement system. Proc. International Workshop on Submillimeter-wave Observation of Earth's Atmosphere from Space (Tokyo, 27-29 January 1999), 169-172.
- Kanzawa, H., Camy-Peyret, C., Kondo, Y., and Papineau, N. (1997): Implementation and first scientific results of the ILAS Validation Balloon Campaign at Kiruna-Esrange in

- February - March 1997. Proc. 13th ESA Symp. European Rocket and Balloon Programmes and Related Research (Oland, Sweden, 26-29 May 1997), ESA SP-397 (September 1997), 211-215.
- Knudsen, B.M., Larsen, N., Mikkelsen, I.S., Morcrette, J.-J., Braathen, G.O., Kyro, E., Fast, H., Gernandt, H., Kanzawa, H., Nakane, H., Dorokhov, V., Yushkov, V., Hansen, G., Gil, M., and Shearman, R.J. (1998): Ozone depletion in and below the Arctic vortex for 1997. *Geophys. Res. Lett.*, 25, No. 5, 627-630.
- Kondo, Y., Koike, M., Engel, A., Schmidt, U., Mueller, M., Sugita, T., Kanzawa, H., Nakazawa, T., Aoki, S., Irie, H., Toriyama, N., Suzuki, T., and Sasano, Y., (1999): NOy-N2O correlation observed inside the Arctic vortex in February 1997: Dynamical and chemical effects. *J. Geophys. Res.*, 104, No. D7, 8215-8224.
- Kreher, K., Bodeker, G.E., Kanzawa, H., Nakane, H., and Sasano, Y. (1999): Ozone and temperature profiles measured above Kiruna inside, at the edge of, and outside the Arctic polar vortex in February and March 1997. *Geophys. Res. Lett.*, 26, No. 6, 715-718.
- Murata, I., N. Fukuma, Y. Ohtaki, H. Fukunishi, H. Kanzawa, H. Nakane, and K. Shibasaki (1999): Measurements of O3 and N2O in Alaska with a tunable diode laser heterodyne spectrometer. *Adv. Space Res.*, in press.
- Sasano, Y., Nakajima, H., Kanzawa, H., Suzuki, M., Yokota, T., Nakane, H., Gernandt, H., Schmidt, A., Herber, A., Yushkov, V., Dorokhov, V., and Deshler, T. (1999a): Validation of ILAS Version 3.10 ozone with ozonesonde measurements. *Geophys. Res. Lett.*, 26, No. 7, 831-834.
- Sasano, Y., Suzuki, M., Yokota, T., and Kanzawa, H. (1999b): Improved Limb Atmospheric Spectrometer (ILAS) for stratospheric ozone layer measurements by solar occultation technique. *Geophys. Res. Lett.*, 26, No. 2, 197-200.
- Sasano, Y., Y. Terao, H. L. Tanaka, T. Yasunari, H. Kanzawa, H. Nakajima, T. Yokota, H. Nakane, S. Hayashida, and N. Saitoh (1999c): ILAS observations of chemical ozone loss in the Arctic stratospheric vortex during early spring 1997. *Geophys. Res. Lett.*, submitted.
- Shibata, T., Y. Iwasaka, M. Fujiwara, M. Hayashi, M. Nagatani, K. Shiraishi, H. Adachi, T. Sakai, K. Susumu, and Y. Nakura (1997): Polar stratospheric clouds observed by lidar over Spitsbergen in the winter of 1994/1995: Liquid particles and vertical "sandwich" structure. *J. Geophys. Res.*, 102, 10829-10840.
- Sugita, T., Y. Kondo, H. Nakajima, U. Schmidt, A. Engel, H. Oelhaf, G. Wetzell, and P.A. Newman (1998): Denitrification observed inside the Arctic vortex in February 1995. *J. Geophys. Res.*, 103, 16221-16233.